A Kinetic Description of Diffusion-Controlled Intramolecular Excimer Formation and Dissociation. 3. Effects of Gibbs Free Energy Changes of Excimer Formation and Sample Imperfections

Guojun Liu

Department of Chemistry, The University of Calgary, 2500 University Drive, NW, Calgary, Alberta, Canada T2N 1N4

Received June 2, 1993; Revised Manuscript Received September 28, 1993®

ABSTRACT: The Liu–Guillet model for diffusion-controlled intramolecular excimer formation and dissociation has been previously used in treating experimental data with success. It has also been deduced to give an expression for the rate constant of excimer formation similar to that derived from the Wilemski–Fixman theory. In this paper, the Liu–Guillet model is shown to be able to explain the quantitative dependence of the rate constant of a diffusion-controlled reaction on its Gibbs free energy change, a capacity unrivaled by any conventional kinetic models in which a diffusion-controlled reaction is deemed to occur as soon as two reactive molecules diffuse into one another within a so-called capture radius R_e. Also examined in this paper is the effect of sample imperfections, i.e., the presence of chains labeled with chromophores at one end only and the presence of a distribution in molar masses of the chains, on the correct recovery of kinetic parameters.

I. Introduction

In the first paper in this series,[1] the Liu–Guillet (L–G) model for describing the kinetics of diffusion-controlled excimer formation from and dissociation into two chromophores, e.g., Py* and Py where Py represents pyrene groups, attached to the opposite ends of a polymer chain has been described in detail. In the model, excimer formation has been assumed to occur due to the coming together of the end groups under the influence of an excimer interaction potential $U(R)$ switched on by exciting one of the end chromophores. The rate of excimer formation according to the model depended on how the end groups of a polymer chain were distributed relative to one another or the end-to-end distance distribution function $P(R)$ at the time of end-group excitation, i.e., at $t = 0$. The closer the end groups are relative to one another at $t = 0$, the faster the rate of excimer formation. Then, the rate depended on the magnitude of the phenomenological relative diffusion coefficient D between the polymer chain ends. The larger the D, the larger is the rate constant. The rate is also related to the shape and depth of the excimer interaction potential $U(R)$. The deeper the potential well or the longer-ranged the attractive part of the interaction potential is, the faster is the rate of excimer formation. The study of the kinetics of excimer formation of end-labeled chains in terms of the L–G model, therefore, should reveal information on $P(R)$, D, and $U(R)$.

Since intramolecular excimer formation in Θ solvents for polymer chains connecting two end chromophores has been discussed, $P(R)$ has been assumed to be Gaussian[2]

$$P(R) = 4\pi R^2\left(\frac{3}{2\pi R_n^{\,2}}\right)^{3/2}\exp\left(\frac{3R^2}{2R_n^{\,2}}\right) \qquad (1)$$

where R_n is the root-mean-square end-to-end distance of the chains. For a chain of finite length m_x, the Gaussian distribution function was normalized so that

$$P'(R) = P(R) = \int_0^{m_x} P(R)\,dR \qquad (2)$$

The excimer interaction potential has been assumed to possess the general form[1]

$$U(R) = -\epsilon_0[2(R_0/R)^n - (R_0/R)^m] \qquad (3)$$

where n, less than m, indicates that the attractive part of the potential is longer-ranged than the repulsive part.

In the second paper of the series,[3] transient monomer and excimer emission intensity profiles $I_M(t)$ and $I_E(t)$ after δ-pulse excitation were computer-generated using the L–G model. The generated curves were then fitted using equations of the Birks scheme:[4]

$$I_M(t) = a_1\exp(-t/\tau_1) + a_2\exp(-t/\tau_2) \qquad (4)$$

and

$$I_E(t) = a_3\exp(-t/\tau_3) + a_4\exp(-t/\tau_4) \qquad (5)$$

In the above equations, a_i's and τ_i's, where i takes values from 1 to 4, are adjustable parameters and are functions of rate constants k_1, k_{-1}, k_M, and k_E of the so-called Birks scheme:

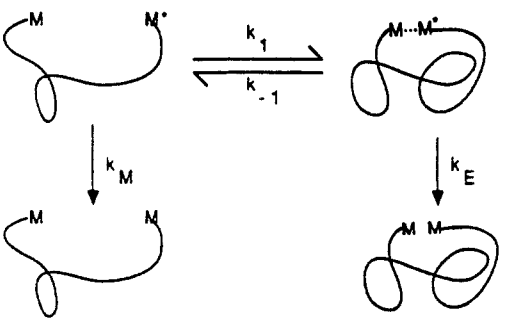

The validity of the Birks scheme in approximating the transient intensity profiles computer-generated using the L–G model was judged by how well the recovered fitting parameters a_i and λ_i, i.e., $1/\tau_i$, satisfy the following relations derived by Birks:[4]

$$a_3 = -a_4 \qquad (6a)$$

$$\lambda_1 = \lambda_3 \qquad (6b)$$

® Abstract published in *Advance ACS Abstracts*, November 1, 1993.

0024-9297/93/2226-6998$04.00/0

$$\lambda_2 = \lambda_4 \tag{6c}$$

When the Birks scheme is valid, the rate constants k_1, k_{-1}, and k_E can be calculated using the following equations:[4]

$$\lambda_1,\lambda_2 = (1/2)\{(Y + X) \mp [(Y - X)^2 + 4k_1k_{-1}]^{1/2}\} \tag{7}$$

and

$$a_2/a_1 = (X - \lambda_1)/(\lambda_2 - X) \tag{8}$$

where

$$X = k_M + k_1 \tag{9}$$

and

$$Y = k_E + k_{-1} \tag{10}$$

Examination of a_i and λ_i parameters obtained from fitting the transient monomer and excimer emission intensity profiles generated using the L–G model demonstrated that equations of the Birks scheme were valid in approximating these transient intensity profiles if the overall deactivation rate of monomers and excimers was slower than the relaxation rate of the polymer chain. The faster chain relaxation criterion was approximately satisfied by the systems, i.e., polystyrene chains of the molecular weight range from 3000 to 10 000 labeled at two ends with pyrene groups, studied by Winnik and coworkers.[5,6] The L–G model thus explained the successful use of equations of the Birks scheme in treating experimental data.

In computing transient monomer and excimer fluorescence intensities of pyrene, n and m values of eq 3 have been assumed to be 3 and 10, respectively. The relation $n = 3$ was established experimentally and theoretically, via quantum mechanic calculations, by Birks et al.[4] for two pyrene groups approaching one another face-to-face with overlapping center axes. It has been previously argued that most pyrene groups in proximity should have face-to-face configurations, because of their thermodynamic favorability and kinetic feasibility.[3] Since the m value would be 12 for two spherical atoms and 8 for two infinitely large parallel planes, two pyrene molecules, each with 16 coplanar carbon and 10 hydrogen atoms approaching one another in the face-to-face configurations, should have an m value between 8 and 12. As previous simulation studies[3] have indicated that m values in the range of 8–12 had little effect on the magnitude of kinetic parameters such as k_1 and k_{-1} recovered, the m value has been arbitrarily chosen to be 10.

Equations of the Liu–Guillet model were then used to fit experimental decay curves monitored by Winnik and co-workers, and reasonable relative end-group diffusion coefficients D were obtained. Furthermore, the rate constants for excimer formation k_1 recovered from analyzing transient monomer and excimer decay data computer-generated using the L–G model obeyed the relation

$$k_1 \propto D/R_n^3 \tag{11}$$

This is in agreement with the Wilemski–Fixman (W–F) theory[7–9] for harmonic spring chains.[10–16] The L–G model was therefore deduced to give an expression similar to that from the W–F theory for the rate constant of intramolecular diffusion-controlled reactions.

In this paper, attention is drawn to one of the major differences between the L–G theory and the W–F theory or any other conventional kinetic theory[17] for diffusion-controlled reactions. In conventional theories, a diffusion-controlled reaction is deemed to occur as soon as two reactive species come within a so-called effective reaction radius R_e. Conventional theories do not provide quantitative predictions as to how R_e and thus the rate constant varies with the Gibbs free energy change ΔG for a reaction. The L–G theory is advantageous in this aspect and can quantitatively predict the dependence of the rate constant of a diffusion-controlled reaction on its Gibbs free energy change.

The other objective of this paper is to examine the effects of sample imperfections on the recovery of kinetic parameters. These imperfections include the presence of polymer chains with chromophores attached to one end only and the unavoidable distribution in the molecular weight of a synthetic polymer. These effects will be examined by generating transient monomer and excimer intensity profiles using the L–G model by taking these imperfections into account, and then the curves will be analyzed using eqs 4 or 5 to see what kinds of results are obtained.

II. Computational Techniques

Generation of Transient Fluorescence Intensity Curves. All computation was done on an IBM RISC system/6000 Model 320 workstation. Transient monomer or excimer intensity curves were generated either by assuming δ-pulse excitation or using a lamp profile measured experimentally. The method for generating transient intensity curves assuming δ-pulse excitation has been described in detail in a previous paper.[3] No noise was added to those curves. Generating transient intensity curves by reading in a lamp profile with an intensity distribution has been described in a more recent publication of the author.[18] Transient intensity curves generated assuming a real lamp profile are made to resemble experimental data by adding Gaussian noise to them.

Transient Fluorescence Intensity Curves for Samples with a Molar Mass Distribution. To generate transient intensity curves of this type, one first has to decide what is a realistic molecular weight distribution function. Polymer samples used for excimer kinetic studies are normally fractionated using gel permeation chromatography (GPC). GPC fractionates polymers according to hydrodynamic volume V_h, which is proportional to hydrodynamic radius R_h cubed, i.e., $V_h \propto R_h^3$. Since R_h and R_n are directly related, a sample fractionated using GPC should usually be Gaussian in shape when plotting $G(R_n)$ versus R_n, where $G(R_n)$ is the probability density function for finding chains with a root-mean-square end-to-end distance R_n. Thus, in accounting for molecular weight distribution, we assumed that there was a Gaussian distribution $G(R_n)$ in R_n

$$G(R_n) \propto \exp\{-[(R_n - \langle R_n\rangle)/\sigma]^2\} \tag{12}$$

where $\langle R_n\rangle$ stands for the average root-mean-square end-to-end distance of a sample, and σ represents the standard deviation in R_n distribution.

For a given $G(R_n)$, one needs to know its molar mass polydispersity. This was achieved by first converting $G(R_n)$ to $f(N)$, the number of repeat units N distribution function, by finding the relation between R_n and N. For the model system, i.e., polystyrene chains end-labeled with pyrene groups, studied in this paper, we assume that all experiments are carried out in a Θ solvent such as cyclohexane at 34.5 °C. In a Θ solvent, R_n of polystyrene chains are related to N by[19]

$$R_n = 5.04N^{0.5}(\text{Å}) \tag{13}$$

After obtaining $f(N)$, the calculation of the polydispersity of a sample from a given $f(N)$ distribution is straightforward.[20]

Table I. Variation of Fitting Parameters and Rate Constants Recovered as a Function of ϵ_0/kT

ϵ_0/kT	a_2/a_1	λ_1 ($\times 10^{-7}$ s)	λ_2 ($\times 10^{-7}$ s)	a_3/a_4	λ_3 ($\times 10^{-7}$ s)	λ_4 ($\times 10^{-7}$ s)	k_{-1} ($\times 10^{-7}$ s)	k_d ($\times 10^{-7}$ s)
2	120.3	33.5	0.443	−0.42	36.7	0.440	31	3.6
3	42.5	22.2	0.469	−0.53	24.4	0.462	20.3	2.5
4	18.0	12.1	0.523	−0.72	12.7	0.517	9.3	2.2
5	7.75	7.25	0.638	−0.81	7.45	0.630	4.6	1.96
6	3.79	4.51	0.827	−0.85	4.54	0.826	1.90	1.85
7	2.02	3.33	1.07	−0.91	3.35	1.07	0.81	1.78
8.45	1.12	2.61	1.39	−0.94	2.62	1.39	0.23	1.74
10	0.35	2.41	1.59	−0.96	2.41	1.59	0.073	1.73
15	0.072	2.62	1.69	−0.95	2.62	1.69	0.025	1.72
20	0.044	2.85	1.70	−0.93	2.86	1.70	0.023	1.72
25	0.030	3.06	1.70	−0.92	3.08	1.70	0.020	1.72

To save computational time, only 11 data points are used to approximate the distribution $G(R_n)$, i.e., starting from $\langle R_n \rangle - (5/2)\sigma$ to $\langle R_n \rangle + (5/2)\sigma$ at a $(1/2)\sigma$ interval. The computation of a set of transient monomer and excimer intensity curves with $\langle R_n \rangle = 40$ Å takes ca. 300 min.

Fitting of Transient Fluorescence Intensity Curves. Transient intensity curves generated by assuming δ-pulse excitation were fitted using a program described previously.[3] Noise-added transient intensity curves generated by assuming a real lamp profile were analyzed using a program purchased from Photon Technology International, Inc.

III. Effect of Gibbs Free Energy Change of a Reaction on Its Rate Constant

Effect of Gibbs Free Energy Change of a Diffusion-Controlled Reaction on Its Rate Constant. The L–G model equates excimer formation to the process of two chromophores coming together under the influence of an excimer interaction potential $U(R)$. The deeper the excimer interaction potential is, the faster is the rate of excimer formation. Since the depth of the interaction potential, characterized by value $-\epsilon_0$, has been assumed to be proportional to the Gibbs free energy change ΔG for excimer formation, the L–G theory predicts a dependence of the rate constant for excimer formation on its free energy change.

To test this dependence, transient monomer and excimer intensity curves were generated assuming δ-pulse excitation for a hypothetical chain with the following chain characteristics: $R_n = 38.6$ Å and $D = 2.0 \times 10^{-6}$ cm²/s. Chromophore characteristic parameters, appropriate for pyrene groups, used included $n = 3$, $m = 10$, $k_M = 4.14 \times 10^6$ s^{-1}, $k_E = 1.72 \times 10^7$ s^{-1}, and $R_0 = 3.6$ Å. Analysis of the transient intensity curves, generated assuming different $-\epsilon_0/kT$ values, using eqs 4 and 5 yielded fitting parameter values a_i and τ_i tabulated in Table I. The rate constants k_1 for excimer formation for different $-\epsilon_0/kT$ values were then calculated from the resulting fitting parameters a_i and τ_i using eqs 7–10.

In Figure 1, the dependence of the rate constant k_1 and $-\epsilon_0/kT$ is illustrated. The rate of excimer formation initially increases rapidly as ϵ_0 increases or $-\epsilon_0/kT$ decreases but levels off as ϵ_0 further increases. There are, unfortunately, no sufficient kinetic data on diffusion-controlled intramolecular excimer formation to verify the theoretical prediction. The L–G model for diffusion-controlled intramolecular reactions can, in principle, be generalized for describing diffusion-controlled intermolecular reactions. The major difference between inter- and intramolecular excimer formation lies in the distance distribution functions $P(R)$ between various chromophores at the time of δ-pulse excitation of the system. For intramolecular excimer formation discussed in this paper, $P(R)$ is given by eq 1. For intermolecular excimer formation, $P(R) \propto 4\pi R^2$. If used for intermolecular reactions, the L–G model

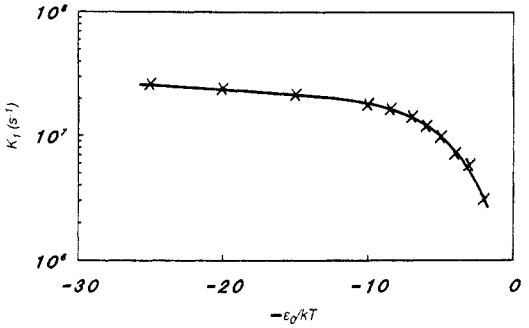

Figure 1. Variation of the rate constant for intramolecular excimer formation as a function of the depth of the excimer interaction potential. The hypothetical polymer chain is assumed to have $R_n = 38.6$ Å and $D = 2.0 \times 10^{-6}$ cm²/s.

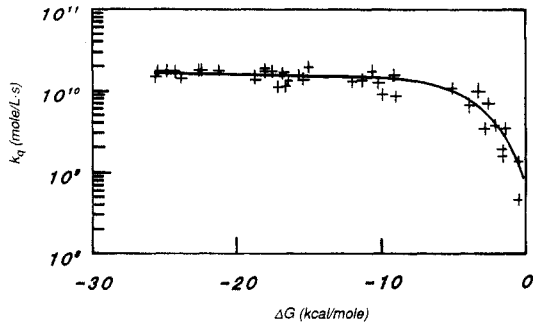

Figure 2. Dependence of the rate constant k_q for diffusion-controlled intermolecular fluorescence quenching reactions on their free energy changes ΔG.

should yield a similar dependence of the rate constant of a diffusion-controlled intermolecular reaction on its Gibbs free energy change. Illustrated in Figure 2 is the dependence of the rate constants k_q for diffusion-controlled intermolecular fluorescence quenching reactions, due to photoinduced electron transfer, on their Gibbs free energy changes measured by Rhem and Weller.[21] Within experimental and computational error, the trends depicted in Figures 1 and 2 are the same. The minor differences between the curves in Figures 1 and 2 are due to different reactions considered in the two cases. It is believed that when the L–G model is used appropriately, i.e., used for the correct reaction type as in this case, a quantitative prediction as to how k_1 varies with ΔG should be possible. This is the strongest feature of the L–G theory when compared to conventional kinetic theories.

The k_1 values corresponding to $-\epsilon_0/kT > -2$ are not included in Figure 1 since, as $-\epsilon_0/kT$ further increases, the process of excimer formation becomes insignificant. Insignificant excimer formation means that the monomer decay is eventually to be single exponential, i.e., characterized by decay constant k_M. That is, one set of the lifetimes τ_1 and τ_3 of eqs 4 and 5 decrease until they become comparable to the time interval between two adjacent data channels so that the τ_i values become unresolvable from the data. The other set, τ_2 and τ_4, approach $1/k_M$ as $-\epsilon_0/$

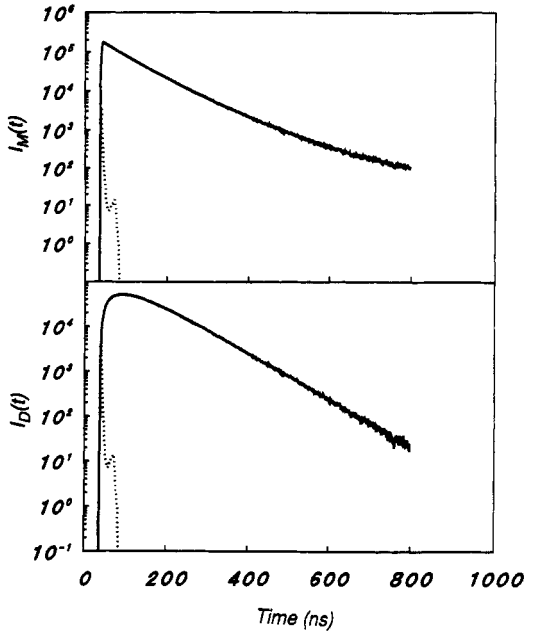

Figure 3. Noise-added transient excimer and monomer fluorescence intensity profiles generated assuming 1% impurity level.

kT increases. This trend is obvious in Table I. In addition, a_1 is seen to decrease rapidly with increasing $-\epsilon_0/kT$.

The use of ϵ_0/kT values smaller than 4 in the generation of transient monomer and excimer intensity profiles led to quite a few consequences. In a previous paper,[22] it has been argued that shortly after pulse excitation several or even more rate constants may be required for describing excimer formation and dissociation, respectively. To obtain the steady-state rate constant for excimer formation or dissociation, transient monomer and excimer intensity profiles should be analyzed starting from a channel which is sufficiently after the pulse excitation channel. The acceptable starting channel for data fitting is determined by plotting τ_i recovered from curve fitting versus the initial data fitting channel number and is taken as the one after which the plot of τ_i versus the initial data fitting channel number levels off. When ϵ_0/kT is small and thus the τ_1 and τ_3 values are small, one cannot skip too many channels after the pulse excitation channel to find the channel after which the plot of τ_i versus the initial data fitting channel number levels off, as after that the $a_1 \exp(-t/\tau_1)$ term of eq 4 may have decayed almost to completion. Thus, fitting data starting from channels which are sufficiently behind the pulse excitation channel was practiced with some arbitrariness but caution when ϵ_0/kT is small. For the $\epsilon_0/kT = 2.0$ case, τ_1 is *ca.* 3.0 ns. Transient monomer and excimer intensity profiles were generated using a very small time increment, i.e., $\Delta t = 0.242$ ns, between adjacent channels. The data were analyzed starting from 0.242 ns after pulse excitation.

Due to the difficulty with locating the best channels for starting data fitting when ϵ_0/kT is small, the recovered τ_i values do not satisfy eqs 6b and 6c with rigor. Because of that, the calculated k_1, k_{-1}, and k_d values are somewhat less accurate than the cases when ϵ_0/kT are larger than 5. The magnitude of relative error expected in k_1 and k_{-1} would probably be comparable with that in k_d. The inputted and thus the recovered k_d values for excimer fluorescence decay should all be 1.72×10^7 s^{-1}.

The other consequence of using small ϵ_0/kT values is that the a_3/a_4 values recovered deviate from -1 significantly as shown in Table I. This should not be of concern, because it is due to the omission of the early channels in data analysis. If early channels are included, the ratio has been demonstrated to approach -1 again.

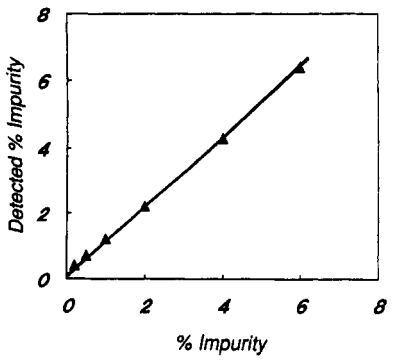

Figure 4. Detected percentage impurity level plotted against inputted percentage impurity level.

Different R_e Values for Excimer Formation of Methyl 4-(1-Pyrenebutyrate) in Different Solvents. Xu and Winnik[23] have recently observed that R_e values for excimer formulation from methyl 4-(1-pyrenebutyrate) are drastically different in solvents toluene (3.28 Å) and cyclohexane (7.27 Å). While this phenomenon is hardly comprehensible in terms of conventional kinetic models, it is perfectly understandable in terms of the L–G model. In terms of the L–G model, this can be accounted for if the Gibbs free energy for excimer formation in cyclohexane is more negative than that in toluene.

While experimental data of ΔG for excimer formation of methyl 4-(1-pyrenebutyrate) are not available in the literature, the use of ΔG for excimer formation of pyrene to approximate those of excimer formation of methyl 4-(1-pyrenebutyrate) in the two solvents has indicated the validity of the prediction by the L–G model. According to Birks and co-workers,[24] the Gibbs free energy of excimer formation for pyrene in cyclohexane at 25 °C should be around $-7.01RT$, where R stands for the gas constant. The enthalpy change ΔH for pyrene excimer formation in toluene measured by Birks and co-workers was −9.2 kcal/mol, whereas that measured by Förster and co-workers[25] was −10.2 kcal/mol. The entropy change ΔS accompanying excimer formation was determined by Förster and co-workers as −22.7 cal/(mol·K). The ΔG value calculated in toluene using $\Delta G = \Delta H - T\Delta S$ and the two sets of ΔH values are either $-4.11RT$ or $-5.76RT$. In either case, the absolute ΔG value is smaller than that in cyclohexane, and thus a smaller R_e in toluene is reasonable.

IV. Effects of Sample Imperfections

Effect of the Presence of Chains Labeled at One End Only. It is experimentally difficult to prepare samples with exactly two pyrene groups attached to the ends of a polymer chain. In real experimental situations, a sample may contain polymer chains which may not have any or one pyrene end only. Chains which do not have pyrene end labels do not affect fluorescence measurement because they do not absorb any incident light. The interference of fluorescence measurement due to the presence of a trace amount of chains with one pyrene end group only will be discussed next.

The presence of a trace amount of impurity chains with one pyrene end group only will not affect the shape of the transient excimer fluorescence intensity curves monitored. This is so because the polymer concentration is assumed to be extremely low and that no intermolecular events occur on the time scale of pyrene fluorescence. The absence of any intermolecular events means that the chains which are labeled at one end only have no contribution to excimer formation.

Due to the lack of intermolecular events, the fluorescence intensity of chains which are labeled at one end only decays

Table II. Variation of Fitting Parameters and Rate Constants as a Function of Polymer Molar Mass Distribution

		monomer				excimer						
σ (Å^{-1})	PD	a_2/a_1	τ_1 (ns^{-1})	τ_2 (ns^{-1})	χ^2	a_3/a_4	τ_4 (ns^{-1})	τ_4 (ns^{-1})	χ^2	k_1 ($\times 10^{-7}$ s)	k_{-1} ($\times 10^{-7}$ s)	k_d ($\times 10^{-7}$ s)
0	1.00	0.949	38.0	72.4	1.02	−0.943	38.6	73.0	1.05	1.60	0.239	1.74
2	1.01	0.855	36.5	72.3	1.05	−0.934	36.9	72.6	1.06	1.69	0.266	1.73
4	1.04	0.818	34.2	74.1	1.09	−0.923	33.9	74.1	1.13	1.81	0.346	1.72
6	1.08	0.795	32.3	77.0	1.36	−0.895	30.9	75.7	1.23	1.93	0.439	1.69
8	1.14	0.776	31.8	81.1	1.93	−0.851	28.4	77.4	1.32	2.01	0.520	1.64

with rate constant k_M. In cases when the Birks scheme is valid, one expects that the fluorescence intensity of monomer in such a system decays after pulse excitation following

$$I_M(t) = a_1 \exp(-t/\tau_1) + a_2 \exp(-t/\tau_2) + a_0 \exp(-k_M t) \quad (14)$$

where a_0 gives the relative one-end-labeled impurity level in the system.

To test the validity of the foregoing argument, transient monomer and excimer intensity curves were generated using an experimentally measured lamp profile and the following parameters: $D = 3.6 \times 10^{-6}$ cm^2/s, $R_n = 50$ Å, $\epsilon_0/kT = 8.45$, $n = 3$, $m = 10$, and $k_M = 4.14 \times 10^6$ s^{-1}, $k_E = 1.72 \times 10^7$ s^{-1}, and $R_0 = 3.6$ Å. Gaussian noise was then added to the generated curves. The noise-added decay curves were analyzed using eqs 4 and 5 by fitting data 22.4 ns after the peak excitation channel to eliminate contributions from higher-order rate constants for excimer formation and dissociation. In Figure 3, the transient monomer and excimer intensity curves for the 1% one-end-labeled impurity case are shown.

As expected, all transient excimer intensity profiles can be fitted using eq 5. The recovered fitting parameters are the same within data fitting error independent of the amount of impurity present.

The use of eq 14 in fitting the generated monomer decay curves yielded lifetimes τ_1, τ_2, and τ_0. The recovered τ_0 value is very close to the inputted fluorescence lifetime of pyrene in the absence of excimer formation. The lifetimes τ_1 and τ_2 satisfy eqs 6b and 6c within fitting error. The recovered amplitude coefficient a_0 was found to be the same as the inputted impurity level. This is illustrated in Figure 4.

Effect of Polydispersity in Molecular Weight Distribution. To see the effect of sample polydispersity on the recovered k_1 and k_{-1} values, transient monomer and excimer fluorescence intensity profiles were generated using the techniques described in the Computational Techniques section. Curves were generated using an experimentally measured lamp profile as the one shown in Figure 3. The other parameters used for data generation included $\langle R_n \rangle = 40$ Å, $D = 2.4 \times 10^{-6}$ cm^2/s, $\epsilon_0/kT = 8.45$, $n = 3$, $m = 10$, $k_M = 4.14 \times 10^6$ s^{-1}, $k_E = 1.72 \times 10^7$ s^{-1}. Gaussian noise was then added to the generated decay curves. The curves were fitted starting from a channel which was 14.4 ns after the peak excitation channel using eqs 4 and 5.

Results of analyzing these generated curves using eqs 4 and 5 are presented in Table II. As sample polydispersity (PD) increases, the Birks scheme, as expected, becomes less satisfactory in interpreting the data. This is reflected in the increased χ^2 value of fitting and in the disagreement between τ_1 and τ_3 or τ_2 and τ_4 values obtained.

As PD increases, the k_1 value increases. This is expected because k_1 does not vary with R_n in a linear fashion. In fact, k_1, in terms of the harmonic spring model, is given by eq 11 and is inversely proportional to the third power of R_n. That is, in calculating the average $\langle k_1 \rangle$ for a polydispersed sample, more emphasis is placed on the chains with lower R_n values but higher rate constants k_1. For a sample which possesses a symmetric $P(R_n)$ distribution, the averaged k_1 value, i.e., $\langle k_1 \rangle$, should have a larger value than that for a sample which is monodispersed with a root-mean-square end-to-end distance equal to $\langle R_n \rangle$. In practical experiments, PD should be in the range of 1.04–1.08. Thus a 10–20% error is expected of the recovered k_1 value.

The increase in k_{-1} with PD was quite a surprise, because results of a previous paper in this series[3] only demonstrated a slight dependence of k_{-1} value on R_n. A closer examination of eqs 7–10 reveals that k_{-1} is obtained as a small number resulting from mathematical operations involving the subtraction of large numbers like $1/\tau_1 - 1/\tau_2$. As the polydispersity increases, eqs 6b and 6c are not satisfied rigorously and thus the uncertainty in τ_1 and τ_2 values increases. The increased uncertainty in τ_1 and τ_2 values may cause errors in the resultant k_{-1} values. Thus, the increase in the recovered k_{-1} values with PD is most likely due to calculation errors. The increased errors in k_{-1} values as PD increases can be partially seen from the erroneous k_d values recovered as PD increases.

V. Conclusions

The Liu–Guillet model for diffusion-controlled intramolecular excimer formation and dissociation has been demonstrated to be superior to conventional kinetic models in its ability to quantitatively predict the change in the rate of such reactions as a function of their free energy changes. It would be interesting to verify the trend depicted in Figure 1 experimentally. This would involve the excimer formation and dissociation kinetic studies of a particular polymer labeled with various chromophores which have different $-\epsilon_0/kT$ values. Alternatively, one may be able to carry out the kinetic study for a particular sample in a series of Θ solvents for the polymer chain. In Θ solvents, the conformation of a particular polymer sample in the absence of end-group perturbance would have the same average conformation. On the other hand, the Gibbs free energy for excimer formation may be different.

The presence of a trace amount of one-end-labeled impurity in a sample used for excimer formation kinetic studies can be easily detected experimentally. The presence of such impurities has been shown not to affect the transient excimer fluorescence intensity profiles. In cases when such impurities are present, it is recommended that one analyze excimer intensity profiles for obtaining kinetic parameters. Last, simulation studies have shown that, for excimer kinetic studies, one should prepare samples with polydispersities below 1.05. When samples of such a polydispersity are used, the recovered k_1 value may be larger than that of a monodispersed sample by ~15%.

Acknowledgment. The author thanks the Natural Sciences and Engineering Research Council of Canada for financial support of this research. The author is grateful to Professor M. A. Winnik of the University of Toronto for suggesting the study of the effect of sample imperfections on the recovered kinetic parameters. Dr.

Winnik is also acknowledged for bringing their R_0 values for methyl 4-(1-pyrenebutyrate) excimer formation in different solvents to the author's attention.

References and Notes

(1) Liu, G. J.; Guillet, J. E. *Macromolecules* **1990**, *23*, 4292.
(2) de Gennes, P.-G. *Scaling Concepts in Polymer Physics*; Cornell University Press: Ithaca, NY, 1979.
(3) Liu, G. J. *Macromolecules* **1992**, *25*, 5805.
(4) Birks, J. B. *Photophysics of Aromatic Molecules*; Wiley-Interscience: New York, 1970.
(5) Winnik, M. A.; Redpath, A. E. C.; Panton, K.; Danhelka, J. *Polymer* **1984**, *25*, 91.
(6) Winnik, M. A. In *Molecular Dynamics in Restricted Geometry*; Klafter, J., Drake, J. M., Eds.; Wiley: New York, 1989.
(7) Wilemski, G.; Fixman, M. *J. Chem. Phys.* **1973**, *58*, 4009.
(8) Wilemski, G.; Fixman, M. *J. Chem. Phys.* **1974**, *60*, 866.
(9) Wilemski, G.; Fixman, M. *J. Chem. Phys.* **1974**, *60*, 878.
(10) Doi, M. *Chem. Phys.* **1975**, *9*, 455.
(11) Sunagawa, S.; Doi, M. *Polym. J.* **1975**, *7*, 604.
(12) Sunagawa, S.; Doi, M. *Polym. J.* **1975**, *8*, 239.
(13) (a) Perico, A.; Cuniberti, C. *J. Polym. Sci., Polym. Phys. Ed.* **1977**, *15*, 1435. (b) Perico, A.; Beggiate, Cuniberti, C. *J. Phys. Chem.* **1975**, *62*, 4911.
(14) (a) Cuniberti, C.; Perico, A. *Prog. Polym. Sci.* **1984**, *10*, 271. (b) Perico, A.; Cuniberti, C. *Macromolecules* **1990**, *23*, 797.
(15) de Gennes, P.-G. *J. Chem. Phys.* **1971**, *55*, 572.
(16) Friedman, B.; O'Shaughnessy, B. *Macromolecules* **1993**, *26*, 4888.
(17) Rice, A. S. In *Comprehensive Chemical Kinetics*; Banford, C. H., Tripper, C. F. H., Compton, R. G., Eds.; Elsevier: New York, 1985.
(18) Liu, G. J. *Macromolecules* **1993**, *26*, 5687.
(19) Brandrup, J.; Immergut, E. H. *Polymer Handbook*, 3rd ed.; Wiley: New York, 1989.
(20) Young, R. J.; Lovell, P. A. *Introduction to Polymers*, 2nd ed.; Chapman & Hall: London, 1991; pp 211–220.
(21) Rehm, D.; Weller, A. *Isr. J. Chem.* **1970**, *8*, 259.
(22) Liu, G. J. *Macromolecules*, in press.
(23) Xu, R. L.; Winnik, M. A. *J. Photochem. Photobiol. A: Chem.* **1991**, *57*, 351.
(24) (a) Birks, J. B.; Braga, C. L.; Lumb, M. D. *Proc. R. Soc. London* **1965**, *A283*, 83. (b) Birks, J. B.; Christophorou, L. G. *Spectrochim. Acta* **1963**, *19*, 401. (c) Birks, J. B.; Lumb, M. D.; Munro, I. H. *Proc. R. Soc. London* **1964**, *A280*, 289.
(25) Förster, Th.; Seidel, H. P. *Z. Phys. Chem. (N.F.)* **1965**, *48*, 58.